

# Quantum key distribution with entangled photon sources

Xiongfeng Ma,<sup>1,\*</sup> Chi-Hang Fred Fung,<sup>1,†</sup> and Hoi-Kwong Lo<sup>1,‡</sup>

<sup>1</sup>*Center for Quantum Information and Quantum Control,  
Department of Electrical & Computer Engineering and Department of Physics,  
University of Toronto, Toronto, Ontario, Canada, M5S 1A7*

## Abstract

A parametric down-conversion (PDC) source can be used as either a triggered single photon source or an entangled photon source in quantum key distribution (QKD). The triggering PDC QKD has already been studied in the literature. On the other hand, a model and a post-processing protocol for the entanglement PDC QKD are still missing. In this paper, we fill in this important gap by proposing such a model and a post-processing protocol for the entanglement PDC QKD. Although the PDC model is proposed to study the entanglement-based QKD, we emphasize that our generic model may also be useful for other non-QKD experiments involving a PDC source. Since an entangled PDC source is a basis independent source, we apply Koashi-Preskill's security analysis to the entanglement PDC QKD. We also investigate the entanglement PDC QKD with two-way classical communications. We find that the recurrence scheme increases the key rate and Gottesman-Lo protocol helps tolerate higher channel losses. By simulating a recent 144km open-air PDC experiment, we compare three implementations — entanglement PDC QKD, triggering PDC QKD and coherent state QKD. The simulation result suggests that the entanglement PDC QKD can tolerate higher channel losses than the coherent state QKD. The coherent state QKD with decoy states is able to achieve highest key rate in the low and medium-loss regions. By applying Gottesman-Lo two-way post-processing protocol, the entanglement PDC QKD can tolerate up to 70dB combined channel losses (35dB for each channel) provided that the PDC source is placed in between Alice and Bob. After considering statistical fluctuations, the PDC setup can tolerate up to 53dB channel losses.

PACS numbers:

---

\*Electronic address: xima@physics.utoronto.ca

†Electronic address: cffung@comm.utoronto.ca

‡Electronic address: hklo@comm.utoronto.ca

## I. INTRODUCTION

There are mainly two types of quantum key distribution (QKD) schemes. One is the prepare-and-measure scheme such as BB84 [1] and the other is the entanglement based QKD such as Ekert91 [2]. The security of both types of QKD has been proven in the last decade, see for example, [3, 4, 5]. For a review of quantum cryptography, one may refer to [6]. Meanwhile, researchers have also proven the security of QKD with realistic devices, such as [7, 8, 9, 10, 11, 12, 13].

In the original proposal of the BB84 protocol, a single photon source is required. Unfortunately, single photon sources are still not commercially available. Instead, a weak coherent state source is widely used as an imperfect single photon source. Throughout this paper, we call this implementation as coherent state QKD. Many coherent state QKD experiments have been performed since the first QKD experiment [14], see for example [15, 16, 17, 18, 19, 20].

Decoy state method [21] has been proposed as a useful method for substantially improving the performance of the coherent state QKD. The security of QKD with decoy states has been proven [22, 23, 24]. Asymptotically, the coherent state QKD with decoy states is able to operate as good as QKD with perfect single photon sources in the sense that the key generation rates given by both setups linearly depend on the channel transmittance [24]. Afterwards, some practical decoy-state protocols are proposed [25, 26, 27, 28]. The experimental demonstrations for decoy state method have been done recently [29, 30, 31, 32, 33, 34]. Other than decoy state method, there are other approaches to enhance the performance of the coherent state QKD, such as QKD with strong reference pulses [35, 36] and differential-phase-shift QKD [37].

Besides the coherent source, there is another source that can be used for QKD — parametric down-conversion (PDC) source. With a PDC source, one can realize either prepare-and-measure or entanglement-based QKD protocols. To implement a prepare-and-measure QKD protocol, one can use a PDC source as a triggered single photon source. To implement an entanglement-based QKD protocol, on the other hand, one can use the polarization entanglement between two modes of the light emitted from a PDC source. We call these two implementations triggering PDC QKD and entanglement PDC QKD. With a entangled source, one can also implement QKD protocols based on causality [38] and Bell's inequality [39].

The model and post-processing of the triggering PDC QKD have already been studied [8]. Recently, there are some practical decoy state proposals for the triggering PDC QKD [40, 41, 42]. In this paper, we will focus on the asymptotic decoy state protocol [24], which is the upper bound of all these practical decoy state protocols when threshold detectors are used by Alice and Bob.

On the other hand, the model and post-processing for the entanglement PDC QKD are still missing. In this paper, we present a model for the entanglement PDC QKD. From the model, we find that an entangled PDC source is a basis independent source for QKD. Based on this observation, we propose a post-processing scheme by applying Koashi-Prekill's security analysis [12].

Recently, a free-space distribution of entangled photons over 144 km has been demonstrated [43]. We simulate this experiment setup and compare three QKD implementations: entanglement PDC QKD, triggering PDC QKD and coherent state QKD. In the simulation, we also apply Gottesman-Lo two-way post-processing protocol [44] and a recurrence scheme [45], see also [46].

The main contributions of this paper are:

- We present a model for the entanglement PDC QKD. Although the model is proposed to study the entanglement-based QKD, this generic model may also be useful for other non-QKD experiments involving a PDC source.
- From the model, we find that an entangled PDC source is a basis independent source for QKD. Based on this observation, we propose a post-processing scheme for the entanglement PDC QKD. Essentially, we apply Koashi-Prekill's security analysis [12].
- By simulating a PDC experiment [43], we compare three QKD implementations: entanglement PDC QKD, triggering PDC QKD and coherent state QKD. In the entanglement PDC QKD, we consider two cases: source in the middle and source at Alice's side.
- In the case that the PDC source is placed in between Alice and Bob, we find that the entanglement PDC QKD can tolerate the highest channel losses, up to 70 dB by applying Gottesman-Lo two-way classical communication post-processing protocol [44]. We remark that a 35dB channel loss is comparable to the estimated loss in a

satellite to ground transmission in the literature [47, 48].

- We consider statistical fluctuations for the entanglement PDC QKD. In this case, the PDC setup can tolerate up to 53dB channel loss.
- The coherent state QKD with decoy states is able to achieve highest key rate in the low- and medium-loss regions.

In Section II, we will review two experiment setups of the entanglement PDC QKD. In Section III, we will model the entanglement PDC QKD. In Appendix A, we calculate the quantum bit error rate in the entanglement PDC QKD. In Section IV, we will propose a post-processing scheme for the entanglement PDC QKD. In Section V, we will compare the entanglement PDC QKD, the triggering PDC QKD and the coherent state QKD by simulating a real PDC experiment. We also apply protocols based on two-way classical communications and consider statistical fluctuations. In Appendix B, we investigate the optimal  $\mu$  for the entanglement PDC QKD.

## II. IMPLEMENTATION

In general, the PDC source does not necessarily belong to one of the two legitimate users of QKD, Alice or Bob. One can even assume that an eavesdropper, Eve, owns the PDC source. In this section we will compare two experimental setups of the entanglement PDC QKD due to the position of the PDC source, in between Alice and Bob or at Alice's side.

Let us start with a general discussion about an entangled PDC source. With the rotating-wave approximation, the Hamiltonian of the PDC process can be written as [49]

$$H = i\chi(a_H^\dagger b_V^\dagger - a_V^\dagger b_H^\dagger) + h.c. \quad (1)$$

where  $h.c.$  means Hermitian conjugate and  $\chi$  is a coupling constant depending on the crystal nonlinearity and the amplitude of the pump beam. The operators  $a_i$  and  $b_i$  are the annihilation operators for rectilinear polarizations  $i \in \{H, V\}$  in mode  $a$  and  $b$  respectively. Mode  $a$  and mode  $b$  are the modes sent to Alice and Bob, respectively.

In the Section III, we will focus on modeling the measurement of the rectilinear polarization ( $Z$ ) basis. Due to symmetry, all the calculations can be applied to  $X$  basis too.

### A. Source in the middle

First we consider the case that the PDC source sits in between Alice and Bob. The schematic diagram is shown in FIG. 1.

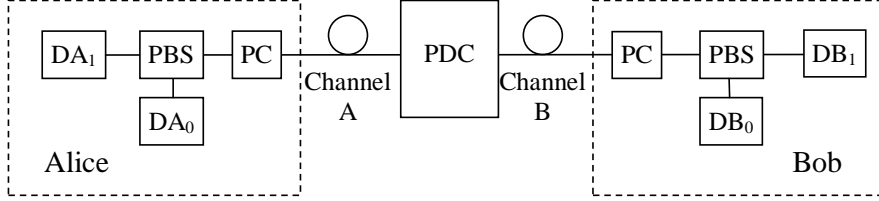


FIG. 1: A schematic diagram for the entanglement PDC QKD. Alice and Bob connect to a entangled PDC source by optical links. They each receives one of two entangled modes coming out from the PDC source. Both Alice and Bob randomly choose basis (by polarization controllers) to measure the arrived signals (by single photon detectors). PC: polarization controller; PBS: polarized beam splitter; DA<sub>0</sub>, DA<sub>1</sub>, DB<sub>0</sub>, DB<sub>1</sub>: threshold detectors.

As shown in FIG. 1, a PDC source provides two entangled modes,  $a$  and  $b$ , which are sent to Alice and Bob, respectively. After receiving the signals, Alice and Bob each randomly chooses a basis ( $X$  or  $Z$ ) to perform a measurement. One key observation of this setup is that the state emitted from the PDC source is independent of the bases Alice and Bob choose for the measurements.

### B. Source at Alice's side

Another case is that Alice owns the PDC source. The schematic diagram is shown in FIG. 2.

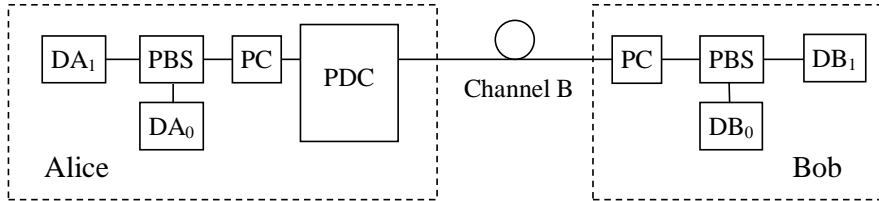


FIG. 2: A schematic diagram for the entanglement PDC QKD. Alice measures one of entangled modes coming out from the PDC source and sends Bob the other mode.

Compare FIG. 1 and 2, we can see that the only difference is the position of the PDC source. As we will see in Section IV, the post-processing these two setups are similar.

We remark that in the second setup, Alice's measurement commutes with Bob's measurement. Thus, we have the same observation as before that the PDC source state is independent of the measurement bases.

Therefore, for both setups the entangled PDC source is a basis-independent source. It follows that the entanglement PDC QKD is a basis independent QKD.

### III. MODEL

In this section, we will model entangled PDC sources, channel and detectors for the entanglement PDC QKD. We emphasize that this model is applicable for both experiment setups described in Section II.

#### A. An entangled PDC source

From Eq. (1), the state emitted from a type-II PDC source can be written as [49]

$$|\Psi\rangle = (\cosh \chi)^{-2} \sum_{n=0}^{\infty} \sqrt{n+1} \tanh^n \chi |\Phi_n\rangle, \quad (2)$$

where  $|\Phi_n\rangle$  is the state of an  $n$ -photon-pair, given by

$$|\Phi_n\rangle = \frac{1}{\sqrt{n+1}} \sum_{m=0}^n (-1)^m |n-m, m\rangle_a |m, n-m\rangle_b. \quad (3)$$

For example, when  $n = 1$ , Eq. (3) will give a Bell state,

$$\begin{aligned} |\Phi_1\rangle &= \frac{1}{\sqrt{2}} (|1, 0\rangle_a |0, 1\rangle_b - |0, 1\rangle_a |1, 0\rangle_b) \\ &= \frac{1}{\sqrt{2}} (|\leftrightarrow\rangle_a |\updownarrow\rangle_b - |\updownarrow\rangle_a |\leftrightarrow\rangle_b), \end{aligned} \quad (4)$$

Here we use the polarizations  $|1, 0\rangle = |\leftrightarrow\rangle$  and  $|0, 1\rangle = |\updownarrow\rangle$  as a qubit basis (Z basis) for QKD. From Eq. (2), the probability to get an  $n$ -photon-pair is

$$P(n) = \frac{(n+1)\lambda^n}{(1+\lambda)^{n+2}} \quad (5)$$

where we define  $\lambda \equiv \sinh^2 \chi$ . The expected photon pair number is  $\mu = 2\lambda$ , which is the average number of photon pairs generated by one pump pulse, characterizing the brightness of a PDC source.

## B. Detection

We assume that the detection probabilities of the photons in the state of Eq. (3) are independent. Define  $\eta_A$  and  $\eta_B$  to be the detection efficiencies for Alice and Bob, respectively. Both  $\eta_A$  and  $\eta_B$  take into account of the channel losses, detector efficiencies, coupling efficiencies and losses inside the detector box. For an  $n$ -photon-pair, the overall transmittance is

$$\eta_n = [1 - (1 - \eta_A)^n][1 - (1 - \eta_B)^n]. \quad (6)$$

We remark that the channel loss is included in  $\eta_A$  and  $\eta_B$ . Thus, this model can be applied to either of following two cases: 1) the PDC source is in between Alice and Bob or 2) the PDC source is at Alice (or Bob)'s side.

**Yield:** define  $Y_n$  to be the yield of an  $n$ -photon-pair, i.e., the conditional probability of a coincidence detection event given that the PDC source emits an  $n$ -photon-pair.  $Y_n$  mainly comes from two parts, the background and the true signal. Assuming that the background counts are independent of the signal photon detection, then  $Y_n$  is given by

$$Y_n = [1 - (1 - Y_{0A})(1 - \eta_A)^n][1 - (1 - Y_{0B})(1 - \eta_B)^n] \quad (7)$$

where  $Y_{0A}$  and  $Y_{0B}$  are the background count rates at Alice's and Bob's sides, respectively. The vacuum state contribution is  $Y_0 = Y_{0A}Y_{0B}$ . The *gain* of the  $n$ -photon-pair  $Q_n$ , which is the product of Eqs. (5) and (7), is given by

$$\begin{aligned} Q_n &= Y_n P(n) \\ &= [1 - (1 - Y_{0A})(1 - \eta_A)^n][1 - (1 - Y_{0B})(1 - \eta_B)^n] \frac{(n+1)\lambda^n}{(1+\lambda)^{n+2}}. \end{aligned} \quad (8)$$

The overall gain is given by

$$\begin{aligned} Q_\lambda &= \sum_{n=0}^{\infty} Q_n \\ &= 1 - \frac{1 - Y_{0A}}{(1 + \eta_A \lambda)^2} - \frac{1 - Y_{0B}}{(1 + \eta_B \lambda)^2} + \frac{(1 - Y_{0A})(1 - Y_{0B})}{(1 + \eta_A \lambda + \eta_B \lambda - \eta_A \eta_B \lambda)^2}. \end{aligned} \quad (9)$$

Here the overall gain  $Q_\lambda$  is the probability of a coincident detection event given a pump pulse. Note that the parameter  $\lambda$  is one half of the expected photon pair number  $\mu$ .

The overall quantum bit error rate (QBER,  $E_\lambda$ ) is given by

$$E_\lambda Q_\lambda = e_0 Q_\lambda - \frac{2(e_0 - e_d)\eta_A \eta_B \lambda (1 + \lambda)}{(1 + \eta_A \lambda)(1 + \eta_B \lambda)(1 + \eta_A \lambda + \eta_B \lambda - \eta_A \eta_B \lambda)} \quad (10)$$

where  $Q_\lambda$  is the gain given in Eq. (9). The calculation of the  $E_\lambda$  is shown in Appendix A.

#### IV. POST-PROCESSING

As mentioned in Section II, the entanglement PDC QKD is a basis-independent QKD. Thus, we can apply Koashi and Preskill's security proof [12]. The key generation rate is given by

$$R \geq q\{Q_\lambda[1 - f(\delta_b)H_2(\delta_b) - H_2(\delta_p)]\}. \quad (11)$$

where  $q$  is the basis reconciliation factor (1/2 for the BB84 protocol due to the fact that half of the time Alice and Bob disagree with the bases, and if one uses the efficient BB84 protocol [50],  $q \approx 1$ ), the subscript  $\lambda$  denotes for one half of the expected photon number  $\mu$ ,  $Q_\lambda$  is the overall gain,  $\delta_b$  ( $\delta_p$ ) is the bit (phase) error rate,  $f(x)$  is the bi-direction error correction efficiency (see, for example, [51]) as a function of error rate, normally  $f(x) \geq 1$  with Shannon limit  $f(x) = 1$ , and  $H_2(x)$  is the binary entropy function,

$$H_2(x) = -x \log_2(x) - (1 - x) \log_2(1 - x).$$

Due to the symmetry of  $X$  and  $Z$  bases measurements, as shown in Section II,  $\delta_b$  and  $\delta_p$  are given by

$$\delta_b = \delta_p = E_\lambda, \quad (12)$$

where  $E_\lambda$  is the overall QBER. This equation is true for the asymptotic limit of an infinitely long key distribution. Later in the Subsection of VC, we will see Eq. (12) may not be true when statistical fluctuations are taken into account.

We remark that in Koashi and Preskill's security proof, the squash model [13] is applied. In the squash model, Alice and Bob project the state onto the qubit Hilbert space before  $X$  or  $Z$  measurements. For more details of the squash model, one can refer to [13]. In the case that Alice owns the PDC source, as discussed in Subsection IIB, the key rate formula of Eq. (11) has been proven [52] to be valid for the QKD with threshold detectors without the squash model, see also [53]. We also notice that this post-processing scheme, Eqs. (11) and (12), can also be derived from the security analysis based on the uncertainty principle [54].

In Eq. (11),  $Q_\lambda$  can be directly measured from a QKD experiment and  $E_\lambda$  can be estimated by error testing. In the simulation shown in Section V, we will use Eqs. (9) and (10).

We remark that the post-processing for the entanglement PDC QKD is simpler than the coherent state QKD and triggering PDC QKD. In the entanglement PDC QKD, all the



parameters needed for the post-processing ( $Q_\lambda$  and  $E_\lambda$ ) can be directly calculated or tested from the measured classical data. In the coherent PDC QKD and the triggering PDC QKD, on the other hand, Alice and Bob need to know the value of some experimental parameters ahead, such as the expected photon number  $\mu$  ( $= 2\lambda$ ), and also need to estimate the gain and error rate of the single photon states  $Q_1$  and  $e_1$ , which make the statistical fluctuation analysis difficult [28].

The post-processing can be further improved by introducing two-way classical communications between Alice and Bob [44, 46]. Also, the adding noise technique may enhance the performance [55].

## V. SIMULATION

In this section, we will first compare three QKD implementations: entanglement PDC QKD, triggering PDC QKD and coherent state QKD. Then we will apply post-processing protocols with two-way classical communications to the entanglement PDC QKD. Finally, we will consider statistical fluctuations.

We deduce experimental parameters from Ref. [43] due to the model given in Subsection III, which are listed in TABLE I. For the coherent state QKD, we use  $\eta_A = 1$  since Alice prepares the states in this case. In the following simulations, we will use  $q = 1/2$  and  $f(E_\mu) = 1.22$  [51].

Repetition rate	Wavelength	$\eta_{Alice}$	$\eta_{Bob}$	$e_d$	$Y_0$
249MHz	710 nm	14.5%	14.5%	1.5%	$6.02 \times 10^{-6}$

TABLE I: Experimental parameters deduced from 144 km PDC experiment [43]. Here we assume Alice and Bob use detectors with same characteristics.  $e_d$  is the intrinsic detector error rate.  $Y_0$  is the background count rate.  $\eta_{Alice}$  ( $\eta_{Bob}$ ) is the detection efficiency in Alice (Bob)'s box, including detector efficiency and internal optical losses. The overall transmittance  $\eta_A$  ( $\eta_B$ ) is the products of Alice (Bob)'s channel transmission efficiency and  $\eta_{Alice}$  ( $\eta_{Bob}$ ).

The optimal expected photon number  $\mu$  of the coherent state QKD has been discussed in Ref. [8, 28]. In Appendix B, we investigate the optimal  $\mu$  ( $2\lambda$ ) for the entanglement PDC QKD. Not surprisingly, we find that the optimal  $\mu$  for the entanglement PDC QKD is in

the order of 1,  $\mu = 2\lambda = O(1)$ . Thus, the key generation rate given in Eq. (11) depends linearly on the channel transmittance.

### A. Comparison of three QKD implementations

In the first simulation, we assume that Alice is able to adjust the expected photon pair number  $\mu$  ( $2\lambda$ , the brightness of the PDC source) in the region of  $[0, 1]$ . Thus, we can optimize  $\mu$  for the entanglement PDC QKD and the triggering PDC QKD. The simulation results are shown in FIG. 3.

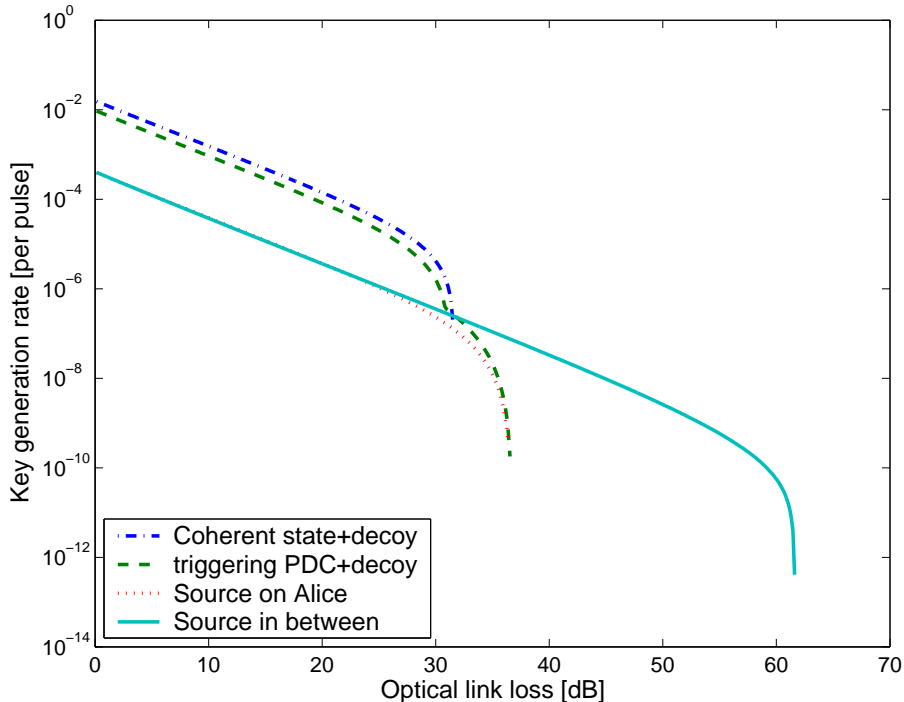


FIG. 3: (Color online) Plot of the key generation rate in terms of the optical loss, comparing comparing four cases: coherent state QKD+asymptotic decoy, triggering PDC+asymptotic decoy, and entanglement PDC QKD (source in the middle and source at Alice’s side). For the coherent state QKD+decoy, we use  $\eta_A = 1$ . We numerically optimize  $\mu$  ( $2\lambda$ ) for each curve.

From FIG. 3, we have the following remarks.

1. The entanglement PDC QKD can tolerate the highest channel losses in the case that the source is placed in middle between Alice and Bob.

2. The coherent state QKD with decoy states is able to achieve the highest key rate in the low- and medium-loss region. This is because in the coherent state QKD implementation, Alice does not need to detect any photons, which will effectively give  $\eta_A = 1$  in the PDC QKD implementations.
3. Comparing two cases of the entanglement PDC QKD: source in the middle and source at Alice's side, they yields similar key rate in the low- and media- region. But source in the middle case can tolerate higher channel losses.

In the following simulations, we will focus on the case that the entangled PDC source sits in the middle between Alice and Bob.

### B. With two-way classical communications

We can also apply the idea of post-processing with two-way classical communications. Similar to the argument of Ref. [46], we combine the recurrence idea [45] and the B steps in the Gottesman-Lo protocol [44]. The simulation results are shown in FIG. 4.

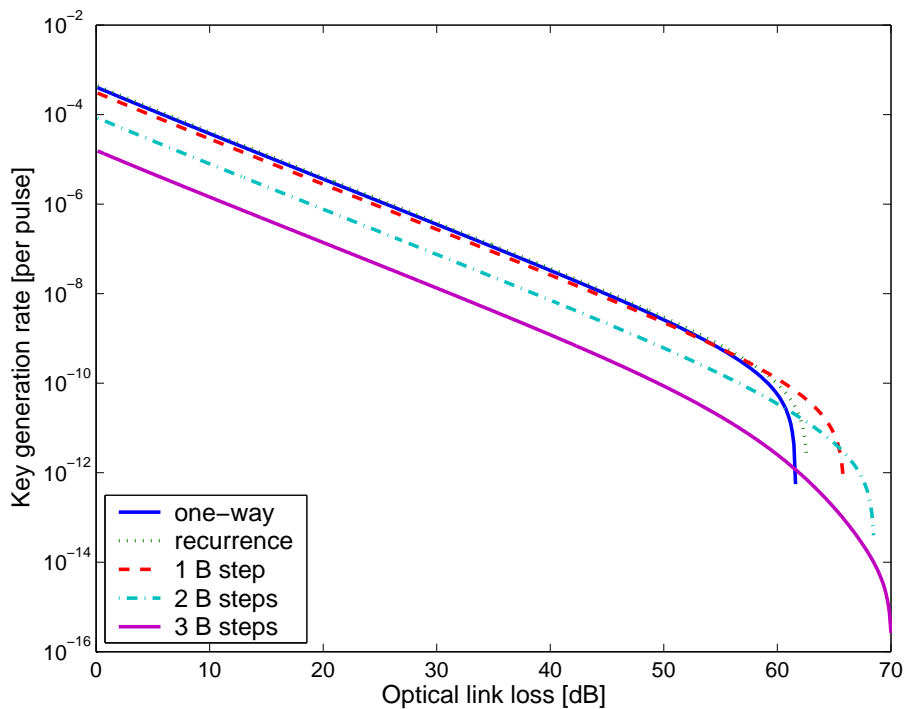


FIG. 4: (Color online) Plot of the key generation rate in terms of the optical loss. We apply the recurrence idea and up to 3 B steps.  $\mu$  is numerically optimized for each curve.

From FIG. 4, we can see that the recurrence scheme can increase the key rate by around 10% and extend the maximal tolerable loss by around 1dB. The PDC experiment setup can tolerate up to 70dB channel loss with 3 B steps. We remark that 70dB (35dB in each channel) is comparable to the estimated loss in a satellite to ground transmission [47, 48]. This result suggests that satellite-ground QKD may be possible. However, this simulation assumes the ideal situation that an infinite number of signals are transmitted. Moreover, we assume that  $\mu$  (the brightness of the PDC source) is a freely adjustable parameter in the PDC experiment. In a more realistic case where a finite number of signals are transmitted and  $\mu$  is a fixed parameter, the tolerable channel loss becomes smaller, as we show next.

### C. Statistical fluctuations

In Eq. (12), we assume that  $\delta_b$  and  $\delta_p$  are the same due to the symmetry between  $X$  and  $Z$  measurements. Alice and Bob randomly choose to measure in  $X$  or  $Z$  basis. Then asymptotically,  $\delta_b$  is good estimate of  $\delta_p$ . However, in a realistic QKD experiment, only a finite number of signals are transmitted. Thus  $\delta_p$  may slightly differ from  $\delta_b$ . We assume that Alice and Bob do not perform error testing explicitly. Instead, they obtain the bit error rate directly from an error correction protocol (e.g., the Cascade protocol [51]). In that case, there is no fluctuation in the bit error rate  $\delta_b = E_\lambda$ . On the other hand, the phase error rate may fluctuate to some certain value  $\delta_p = \delta_b + \epsilon$ . Following the fluctuation analysis of Ref. [5], we know that the probability to get a  $\epsilon$  bias is

$$P_\epsilon \leq \exp\left[-\frac{\epsilon^2 n}{4\delta_b(1-\delta_b)}\right], \quad (13)$$

where  $n = NQ_\lambda$  the number of detection events, the product of total number of pulses  $N$  and the overall gain  $Q_\lambda$ .

In the 144km PDC experiment [43], the repetition rate of pump pulse is 249MHz as given in TABLE I. As discussed in Ref. [48], the typical time of ground-satellite QKD allowed by satellite visibility is 40 minutes. Here, we assume the experiment runs 10 minutes, which means the data size is  $N = 1.5 \times 10^{11}$ . By taking this data size, we consider the fluctuations for the entanglement PDC QKD.

In the realistic case, the brightness of the PDC source  $\mu$  cannot be set freely. In the 144 km PDC experiment [43], the expected photon pair number is  $\mu = 2\lambda = 0.053$ . After taking

$\mu = 0.053$  and the data size of  $N = 1.5 \times 10^{11}$  for the fluctuation analysis, the simulation result is shown in FIG. 5.

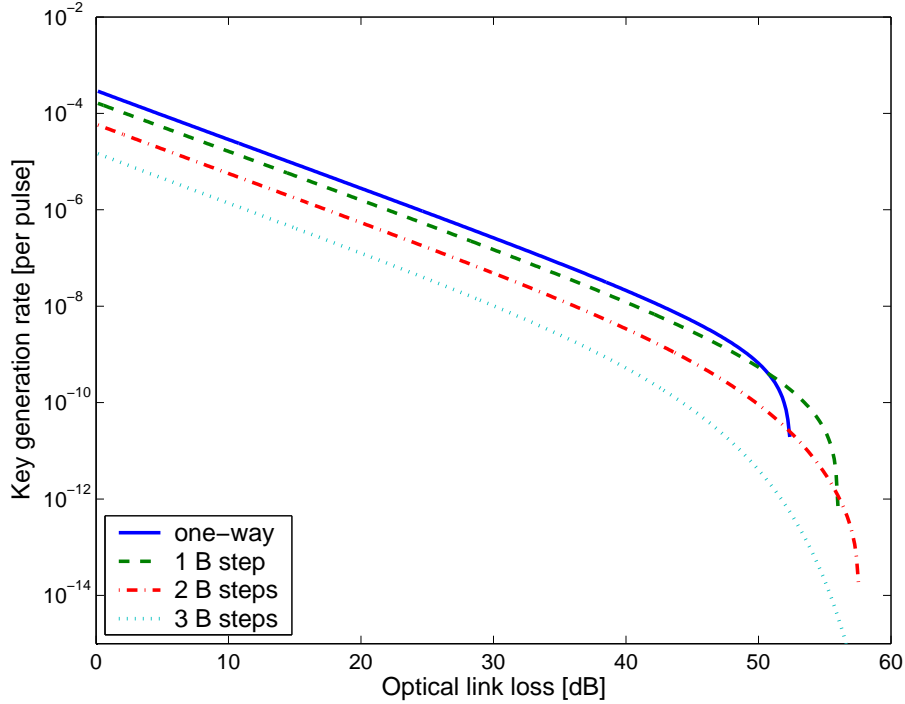


FIG. 5: (Color online) Plot of the key generation rate in terms of the optical loss. We take a realistic  $\mu = 2\lambda = 0.053$ , and consider the fluctuation with a data size of  $N = 1.5 \times 10^{11}$  and a confident interval of  $1 - P_\epsilon \geq 1 - e^{-50}$ .

We have a couple remarks on FIG. 5.

1. In FIG. 5, if we cut off from the key rate of  $10^{-10}$  [57], the entanglement PDC QKD with one B step can tolerate up to 53dB transmission loss.
2. We have tried simulations with various  $\mu$ 's. We find that the key rate is stable with moderate changes of  $\mu$ . With above fluctuation analysis, if we numerically optimize  $\mu$  for each curve, the maximal tolerable channel loss (with cut off key rate of  $10^{-10}$ ) is only 1dB larger than the one given by  $\mu = 0.053$ . Thus, one cannot significantly improve the maximal tolerable channel loss by just using a better PDC source in the 144km PDC experiment setup [43].

## VI. CONCLUSION

We have proposed a model and post-processing for the entanglement PDC QKD. We find that the post-processing is simple by applying Koashi-Preiskill's security proof due to the fact that the entanglement PDC QKD is a basis independent QKD. Specifically, only directly measured data (the overall gain and the overall QBER) are needed to perform the post-processing. By simulating a recent experiment, we compare three QKD schemes: coherent state QKD+asymptotic decoy, triggering PDC+asymptotic decoy, and entanglement PDC QKD (source in the middle and at Alice's side). We find that a) the entanglement PDC (with source in the middle) can tolerate the highest channel loss; b) the coherent state QKD with decoy states can achieve the highest key rate in the medium- and low-loss regions; c) asymptotically, with a realistic PDC experiment setup, the entanglement PDC QKD can tolerate up to 70 dB channel losses by applying post-processing schemes with two-way classical communications; d) the PDC setup can tolerate up to 53 dB channel losses when statistical fluctuations are taken into account.

## VII. ACKNOWLEDGMENTS

We thank R. Adamson, C. Erven, A. M. Steinberg and G. Weihs for enlightening discussions. This work has been supported by CFI, CIAR, CIPI, Connaught, CRC, MITACS, NSERC, OIT, PREA and the University of Toronto. This research is supported by Perimeter Institute for Theoretical Physics. Research at Perimeter Institute is supported in part by the Government of Canada through NSERC and by the province of Ontario through MEDT. X. Ma gratefully acknowledges Chinese Government Award for Outstanding Self-financed Students Abroad. C.-H. F. Fung gratefully acknowledges the Walter C. Sumner Memorial Fellowship and the Shahid U.H. Qureshi Memorial Scholarship.

## APPENDIX A: QUANTUM BIT ERROR RATE

Here we will study the quantum bit error rate (QBER) of the entanglement PDC QKD. Our objective is to derive the QBER formula given in Eq. (10) used in the simulation. The QBER has three main contributions:

1. background counts, which are random noises  $e_0 = 1/2$ ;
2. intrinsic detector errors,  $e_d$ , which is the probability that a photon hit the erroneous detector.  $e_d$  characterizes the alignment and stability of the optical system between Alice's and Bob's detection systems;
3. errors introduced by multi-photon-pair states: a) Alice and Bob may detect different photon pairs; b) double clicks. Due to the strong pulsing attack [56], we assume that Alice and Bob will assign a random bit when they get a double click. In either case, the error rate will be  $e_0 = 1/2$ .

Let us start with the single-photon-pair case, a Bell state given in Eq. (4). The error rate of single-photon-pair  $e_1$  has two sources: background counts and intrinsic detector errors,

$$e_1 = e_0 - \frac{(e_0 - e_d)\eta_A\eta_B}{Y_1} \quad (\text{A1})$$

If we neglect the case that both background and true signal cause clicks, then  $e_1$  can be written as

$$e_1 \approx \frac{e_0(Y_{0A}Y_{0B} + Y_{0A}\eta_B + \eta_A Y_{0B}) + e_d\eta_A\eta_B}{Y_1}. \quad (\text{A2})$$

where  $e_0 = 1/2$  is the error rate of background counts. The first term of the numerator is the background contribution and the second term comes from the errors of true signals.

In the following, we will discuss the errors introduced by multi-photon pair states,  $e_n$  with  $n \geq 2$ . Here we assume Alice and Bob use threshold detectors, which can only tell whether the incoming state is vacuum or non-vacuum. One can imagine the detection of an  $n$ -photon-pair state as follows.

1. Alice and Bob project the  $n$ -photon-pair state, Eq. (3), into  $Z^{\otimes n}$  basis.
2. Afterwards, they detect each photon with certain probabilities ( $\eta_A$  for Alice and  $\eta_B$  for Bob).
3. If either Alice or Bob detects vacuum, then we regard it as a *loss*. If Alice and Bob both detect non-vacuum only in one polarization ( $\leftrightarrow$  or  $\updownarrow$ ), we regard it as a *single click* event. Otherwise, we regard it as a *double click* event.

The state of a 2-photon-pair state, according to Eq. (3), can be written as

$$\begin{aligned}
|\Phi_2\rangle &= \frac{1}{\sqrt{3}}(|2,0\rangle_a|0,2\rangle_b - |1,1\rangle_a|1,1\rangle_b + |0,2\rangle_a|2,0\rangle_b) \\
&= \frac{1}{\sqrt{3}}[|\leftrightarrow\leftrightarrow\rangle_a|\uparrow\uparrow\rangle_b - \frac{1}{2}(|\leftrightarrow\uparrow\rangle + |\uparrow\leftrightarrow\rangle)_a \otimes (|\uparrow\leftrightarrow\rangle + |\leftrightarrow\uparrow\rangle)_b + |\uparrow\uparrow\rangle_a|\leftrightarrow\leftrightarrow\rangle_b].
\end{aligned} \tag{A3}$$

As discussed above, Alice and Bob project the state into  $Z \otimes Z$  basis. If they end up with the first or the third state in the bracket of Eq. (A3), they will get perfect anti-correlation, which will not contribute to errors. If they get the second state in the bracket of Eq. (A3), their results are totally independent, which will cause an error with probability  $e_0 = 1/2$ . Thus the error probability introduced by a 2-photon-pair state is  $1/6$ . Here we have only considered the errors introduced by multi photon states, item 3 discussed in the beginning of this Appendix. We should also take into account the effects of background counts and intrinsic detector errors. With these modifications, the error rate of 2-photon-pair state is given by

$$e_2 = e_0 - \frac{2(e_0 - e_d)[1 - (1 - \eta_A)^2][1 - (1 - \eta_B)^2]}{3Y_2} \tag{A4}$$

where  $Y_2$  is given in Eq. (7). Eq. (A4) can be understood as follows. Only when Alice and Bob project the Eq. (A3) into  $|\leftrightarrow\leftrightarrow\rangle_a|\uparrow\uparrow\rangle_b$  or  $|\uparrow\uparrow\rangle_a|\leftrightarrow\leftrightarrow\rangle_b$  and no background count occurs, they have a probability of  $e_d$  to get the wrong answer. Given a coincident detection, the conditional probability for this case is  $2[1 - (1 - \eta_A)^2][1 - (1 - \eta_B)^2]/3Y_2$ . All other cases, a background count, a double click and measuring different photon pairs, will contribute an error probability  $e_0 = 1/2$ .

Next, let us study the errors coming from the state  $|n - m, m\rangle_a|m, n - m\rangle_b$ . When Alice detects at least one of  $n - m$   $|\uparrow\rangle$  photons but none of  $m$   $|\leftrightarrow\rangle$  photons, and Bob detects at least one of  $n - m$   $|\leftrightarrow\rangle$  photons but none of  $m$   $|\uparrow\rangle$  photons, or both Alice and Bob have bit flips of this case, they will end up with an error probability of  $e_d$ . Given a coincident detection, the conditional probability for these two cases is

$$\begin{aligned}
&\frac{1}{Y_n}\{[1 - (1 - \eta_A)^{n-m}](1 - \eta_A)^m[1 - (1 - \eta_B)^{n-m}](1 - \eta_B)^m \\
&\quad + [1 - (1 - \eta_A)^m](1 - \eta_A)^{n-m}[1 - (1 - \eta_B)^m](1 - \eta_B)^{n-m}\}.
\end{aligned}$$

When Alice detects at least one of  $n - m$   $|\uparrow\rangle$  polarizations but none of  $m$   $|\leftrightarrow\rangle$  polarizations, and Bob detects at least one of  $m$   $|\uparrow\rangle$  polarizations but none of  $n - m$   $|\leftrightarrow\rangle$  polarizations, or both Alice and Bob have bit flips of this case, they will end up with an error probability



of  $1 - e_d$ . Given a coincident detection, the conditional probability for these two case is

$$\begin{aligned} & \frac{1}{Y_n} \{ [1 - (1 - \eta_A)^m] (1 - \eta_A)^{n-m} [1 - (1 - \eta_B)^{n-m}] (1 - \eta_B)^m \\ & + [1 - (1 - \eta_A)^{n-m}] (1 - \eta_A)^m [1 - (1 - \eta_B)^m] (1 - \eta_B)^{n-m} \}. \end{aligned}$$

For all other cases, the error probability is  $e_0$ . Thus the error probability for the state  $|n - m, m\rangle_a |m, n - m\rangle_b$  is

$$\begin{aligned} e_{nm} &= e_0 - \frac{e_0 - e_d}{Y_n} \{ (1 - \eta_A)^{n-m} (1 - \eta_B)^{n-m} [1 - (1 - \eta_A)^m] [1 - (1 - \eta_B)^m] \\ & + (1 - \eta_A)^m (1 - \eta_B)^m [1 - (1 - \eta_A)^{n-m}] [1 - (1 - \eta_B)^{n-m}] \\ & - (1 - \eta_A)^{n-m} (1 - \eta_B)^m [1 - (1 - \eta_A)^m] [1 - (1 - \eta_B)^{n-m}] \\ & - (1 - \eta_A)^m (1 - \eta_B)^{n-m} [1 - (1 - \eta_A)^{n-m}] [1 - (1 - \eta_B)^m] \} \\ & = e_0 - \frac{e_0 - e_d}{Y_n} [(1 - \eta_A)^{n-m} - (1 - \eta_A)^m] [(1 - \eta_B)^{n-m} - (1 - \eta_B)^m] \end{aligned} \quad (\text{A5})$$

In general, for an  $n$ -photon-pair state described by Eq. (3), the error rate is given by

$$\begin{aligned} e_n &= \frac{1}{n+1} \sum_{m=0}^n e_{nm} \\ &= \frac{1}{n+1} \sum_{m=0}^n e_0 - \frac{e_0 - e_d}{Y_n} [(1 - \eta_A)^{n-m} - (1 - \eta_A)^m] [(1 - \eta_B)^{n-m} - (1 - \eta_B)^m] \\ &= e_0 - \frac{e_0 - e_d}{(n+1)Y_n} \sum_{m=0}^n [(1 - \eta_A)^{n-m} - (1 - \eta_A)^m] [(1 - \eta_B)^{n-m} - (1 - \eta_B)^m] \\ &= e_0 - \frac{2(e_0 - e_d)}{(n+1)Y_n} \left[ \frac{1 - (1 - \eta_A)^{n+1} (1 - \eta_B)^{n+1}}{1 - (1 - \eta_A)(1 - \eta_B)} - \frac{(1 - \eta_A)^{n+1} - (1 - \eta_B)^{n+1}}{\eta_B - \eta_A} \right] \end{aligned} \quad (\text{A6})$$

The overall QBER is given by

$$\begin{aligned} E_\lambda Q_\lambda &= \sum_{n=0}^{\infty} e_n Y_n P(n) \\ &= e_0 Q_\lambda - \sum_{n=0}^{\infty} \frac{2(e_0 - e_d) \lambda^n}{(1 + \lambda)^{n+2}} \left[ \frac{1 - (1 - \eta_A)^{n+1} (1 - \eta_B)^{n+1}}{1 - (1 - \eta_A)(1 - \eta_B)} - \frac{(1 - \eta_A)^{n+1} - (1 - \eta_B)^{n+1}}{\eta_B - \eta_A} \right] \\ &= e_0 Q_\lambda - \frac{2(e_0 - e_d) \eta_A \eta_B \lambda (1 + \lambda)}{(1 + \eta_A \lambda)(1 + \eta_B \lambda)(1 + \eta_A \lambda + \eta_B \lambda - \eta_A \eta_B \lambda)} \end{aligned} \quad (\text{A7})$$

where  $Q_\lambda$  is the gain given in Eq. (9).

## APPENDIX B: OPTIMAL $\mu$

The optimal  $\mu$  for the coherent state QKD has already been discussed [8, 28]. Here we need to find out the optimal  $\mu$  for the entanglement PDC QKD. In the following calculation, we will focus on optimizing the parameter  $\lambda$  ( $= \mu/2$ ) for the key generation rate given in Eq. (11).

By assuming  $\eta_B$  to be small and neglecting  $Y_0$ , we can simplify Eq. (9)

$$Q_\lambda \approx 2\eta_B \lambda \left[ 1 - \frac{1 - \eta_A}{(1 + \eta_A \lambda)^3} \right]. \quad (\text{B1})$$

The overall QBER given in Eq. (10) can be simplified to

$$E_\lambda \approx \frac{1}{2} - \frac{(1 - 2e_d)(1 + \lambda)(1 + \eta_A \lambda)}{2(1 + 3\lambda + 3\eta_A \lambda^2 + \eta_A^2 \lambda^3)}. \quad (\text{B2})$$

In order to maximize the key generation rate, given by Eq. (11), the optimal  $\lambda$  satisfies

$$\frac{\partial Q_\lambda}{\partial \lambda} [1 - (1 + f(E_\lambda))H_2(E_\lambda)] - Q_\lambda [1 + f(E_\lambda)] \frac{\partial E_\lambda}{\partial \lambda} \log_2 \frac{1 - E_\lambda}{E_\lambda} = 0. \quad (\text{B3})$$

Here we treat  $f(E_\lambda)$  as a constant. In the following we will consider two extremes:  $\eta_A \approx 1$  and  $\eta_A \ll 1$ .

When  $\eta_A \approx 1$ , the overall gain and QBER are given by

$$\begin{aligned} Q_\lambda &\approx 2\eta_B \lambda \\ E_\lambda &\approx \frac{2e_d + \lambda}{2 + 2\lambda}. \end{aligned} \quad (\text{B4})$$

Thus, Eq. (B3) can be simplified to

$$1 - [1 + f(E_\lambda)]H_2(E_\lambda) - \lambda [1 + f(E_\lambda)] \frac{1 - 2e_d}{2(1 + \lambda)^2} \log_2 \frac{1 - E_\lambda}{E_\lambda} = 0. \quad (\text{B5})$$

When  $\eta_A \ll 1$ ,

$$\begin{aligned} Q_\lambda &\approx 2\eta_A \eta_B \lambda (1 + 3\lambda) \\ E_\lambda &\approx \frac{e_d + \lambda + e_d \lambda}{1 + 3\lambda}. \end{aligned} \quad (\text{B6})$$

Thus, Eq. (B3) can be simplified to

$$(1 + 6\lambda) \{ 1 - [1 + f(E_\lambda)]H_2(E_\lambda) \} - \lambda [1 + f(E_\lambda)] \frac{1 - 2e_d}{1 + 3\lambda} \log_2 \frac{1 - E_\lambda}{E_\lambda} = 0. \quad (\text{B7})$$

The solutions to Eqs. (B5) and (B7) are shown in FIG. 6.

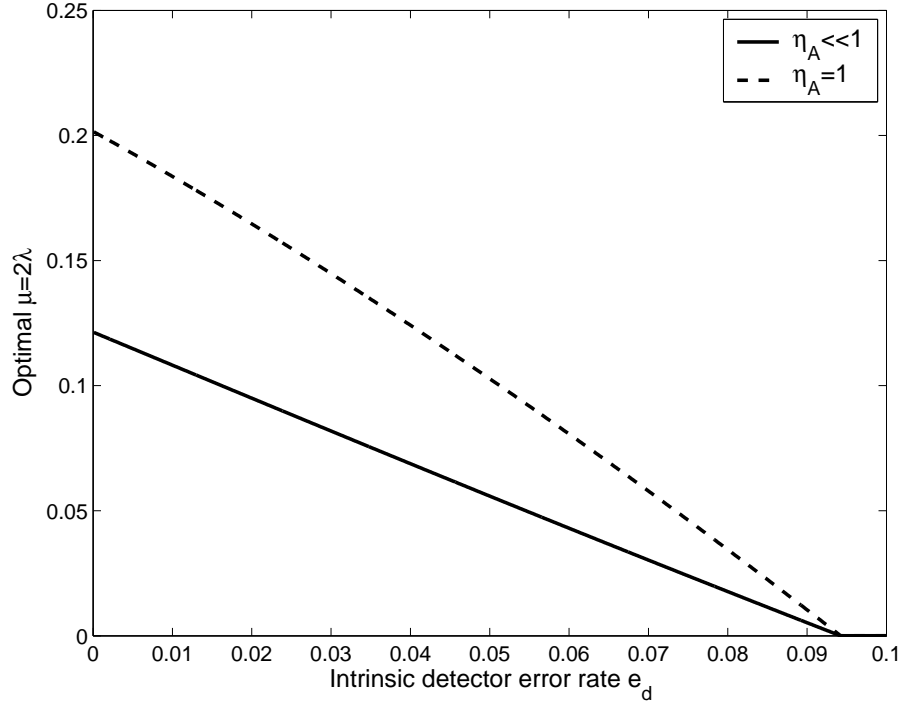


FIG. 6: Plot of the optimal  $\mu$  in terms of  $e_d$  for the entanglement PDC QKD.  $f(e_d) = 1.22$ .

From FIG. 6, we can see that the optimal  $\mu = 2\lambda$  for the entanglement PDC is in the order of 1,  $\mu = 2\lambda = O(1)$ , which will lead the final key generation rate to be  $R = O(\eta_A \eta_B)$ .

- 
- [1] C. H. Bennett and G. Brassard, “Quantum cryptography: Public key distribution and coin tossing,” in *Proceedings of IEEE International Conference on Computers, Systems, and Signal Processing*, (Bangalore, India), pp. 175–179, IEEE, New York, 1984.
  - [2] A. K. Ekert, “Quantum cryptography based on bell’s theorem,” *Phys. Rev. Lett.* , vol. 67, p. 661, 1991.
  - [3] D. Mayers, “Unconditional security in quantum cryptography,” *Journal of the ACM*, vol. 48, p. 351406, May 2001.
  - [4] H.-K. Lo and H.-F. Chau, “Unconditional security of quantum key distribution over arbitrarily long distances,” *Science*, vol. 283, p. 2050, 1999.
  - [5] P. W. Shor and J. Preskill, “Simple proof of security of the BB84 quantum key distribution protocol,” *Phys. Rev. Lett.* , vol. 85, p. 441, July 2000.
  - [6] N. Gisin, G. Ribordy, W. Tittel, and H. Zbinden, “Quantum cryptography,” *Rev. of*

- Mod. Phys.*, vol. 74, pp. 145–195, JANUARY 2002.
- [7] D. Mayers and A. Yao, “Quantum cryptography with imperfect apparatus,” in *FOCS, 39th Annual Symposium on Foundations of Computer Science*, p. 503, IEEE, Computer Society Press, Los Alamitos, 1998.
- [8] N. Lütkenhaus, “Security against individual attacks for realistic quantum key distribution,” *Phys. Rev. A*, vol. 61, p. 052304, 2000.
- [9] G. Brassard, N. Lütkenhaus, T. Mor, and B. Sanders, “Security aspects of practical quantum cryptography,” *Phys. Rev. Lett.*, vol. 85, p. 1330, 2000.
- [10] S. Félix, N. Gisin, A. Stefanov, and H. Zbinden, “Faint laser quantum key distribution: eavesdropping exploiting multiphoton pulses,” *Journal of Modern Optics*, vol. 48, no. 13, p. 2009, 2001.
- [11] H. Inamori, N. Lütkenhaus, and D. Mayers, “Unconditional security of practical quantum key distribution,” *quant-ph/0107017*, 2001.
- [12] M. Koashi and J. Preskill, “Secure quantum key distribution with an uncharacterized source,” *Phys. Rev. Lett.*, vol. 90, p. 057902, 2003.
- [13] D. Gottesman, H.-K. Lo, N. Lütkenhaus, and J. Preskill, “Security of quantum key distribution with imperfect devices,” *Quantum Information and Computation*, vol. 4, p. 325, 2004.
- [14] C. H. Bennett, F. Bessette, G. Brassard, L. Salvail, and J. A. Smolin, “Experimental quantum cryptography,” *Journal of Cryptology*, vol. 5, no. 1, pp. 3–28, 1992.
- [15] P. D. Townsend, “Experimental investigation of the performance limits for first telecommunications-window quantum cryptography systems,” *IEEE Photonics Technology Letters*, vol. 10, pp. 1048–1050, July 1998.
- [16] G. Ribordy, J.-D. Gautier, N. Gisin, O. Guinnard, and H. Zbinden, “Automated ”plug & play” quantum key distribution,” *Electronics Letters*, vol. 34, no. 22, pp. 2116–2117, 1998.
- [17] M. Bourennane, F. Gibson, A. Karlsson, A. Hening, P. Jonsson, T. Tsegaye, D. Ljunggren, and E. Sundberg, “Experiments on long wavelength (1550nm) ”plug and play” quantum cryptography systems,” *Optical Express*, vol. 4, pp. 383–387, May 1999.
- [18] C. Kurtsiefer, P. Zarda, M. Halder, H. Weinfurter, P. M. Gorman, P. R. Tapster, and J. G. Rarity, “Quantum cryptography: A step towards global key distribution,” *Nature*, vol. 419, p. 450, 2002.
- [19] C. Gobby, Z. L. Yuan, and A. J. Shields, “Quantum key distribution over 122 km of standard

- telecom fiber,” *Appl. Phys. Lett.*, vol. 84, pp. 3762–3764, 2004.
- [20] X.-F. Mo, B. Zhu, Z.-F. Han, Y.-Z. Gui, and G.-C. Guo, “Faraday-michelson system for quantum cryptography,” *Optics Letters*, vol. 30, p. 2632, 2005.
- [21] W.-Y. Hwang, “Quantum key distribution with high loss: Toward global secure communication,” *Phys. Rev. Lett.*, vol. 91, p. 057901, August 2003.
- [22] H.-K. Lo, “Quantum key distribution with vacua or dim pulses as decoy states,” in *Proc. of IEEE ISIT*, p. 137, IEEE, 2004.
- [23] X. Ma, “Security of quantum key distribution with realistic devices,” *arXiv: quant-ph/0503057*, 2004.
- [24] H.-K. Lo, X. Ma, and K. Chen, “Decoy state quantum key distribution,” *Phys. Rev. Lett.*, vol. 94, p. 230504, June 2005.
- [25] X.-B. Wang, “Beating the pns attack in practical quantum cryptography,” *Phys. Rev. Lett.*, vol. 94, p. 230503, 2005.
- [26] J. W. Harrington, J. M. Ettinger, R. J. Hughes, and J. E. Nordholt, “Enhancing practical security of quantum key distribution with a few decoy states,” *ArXiv.org:quant-ph/0503002*, 2005.
- [27] X.-B. Wang, “A decoy-state protocol for quantum cryptography with 4 intensities of coherent states,” *Phys. Rev. A*, vol. 72, p. 012322, 2005.
- [28] X. Ma, B. Qi, Y. Zhao, and H.-K. Lo, “Practical decoy state for quantum key distribution,” *Phys. Rev. A*, vol. 72, p. 012326, July 2005.
- [29] Y. Zhao, B. Qi, X. Ma, H.-K. Lo, and L. Qian, “Experimental quantum key distribution with decoy states,” *Phys. Rev. Lett.*, vol. 96, p. 070502, FEBRUARY 2006.
- [30] Y. Zhao, B. Qi, X. Ma, H.-K. Lo, and L. Qian, “Simulation and implementation of decoy state quantum key distribution over 60km telecom fiber,” in *Proc. of IEEE ISIT*, pp. 2094–2098, IEEE, 2006.
- [31] D. Rosenberg, J. W. Harrington, P. R. Rice, P. A. Hiskett, C. G. Peterson, R. J. Hughes, A. E. Lita, S. W. Nam, and J. E. Nordholt, “Long-distance decoy-state quantum key distribution in optical fiber,” *Physical Review Letters*, vol. 98, p. 010503, 2007.
- [32] T. Schmitt-Manderbach, H. Weier, M. Fürst, R. Ursin, F. Tiefenbacher, T. Scheidl, J. Perdigues, Z. Sodnik, C. Kurtsiefer, J. G. Rarity, A. Zeilinger, and H. Weinfurter, “Experimental demonstration of free-space decoy-state quantum key distribution over 144 km,”

- Physical Review Letters*, vol. 98, p. 010504, 2007.
- [33] C.-Z. Peng, J. Zhang, D. Yang, W.-B. Gao, H.-X. Ma, H. Yin, H.-P. Zeng, T. Yang, X.-B. Wang, and J.-W. Pan, “Experimental long-distance decoy-state quantum key distribution based on polarization encoding,” *Physical Review Letters*, vol. 98, p. 010505, 2007.
- [34] Z. L. Yuan, A. W. Sharpe, and A. J. Shields, “Unconditionally secure one-way quantum key distribution using decoy pulses,” *Applied Physics Letters*, vol. 90, p. 011118, 2007.
- [35] M. Koashi, “Unconditional security of coherent-state quantum key distribution with a strong phase-reference pulse,” *Phys. Rev. Lett.* , vol. 93, p. 120501, September 2004.
- [36] K. Tamaki, N. Lütkenhaus, M. Koashi, and J. Batuwantudawe, “Unconditional security of the bennett 1992 quantum key-distribution scheme with strong reference pulse,” *arXiv:quant-ph/0607082*, 2006.
- [37] K. Inoue, E. Waks, and Y. Yamamoto, “Differential phase shift quantum key distribution,” *Phys. Rev. Lett.* , vol. 89, p. 037902, 2002.
- [38] L. Masanes and A. Winter, “Unconditional security of key distribution from causality constraints,” *ArXiv: quant-ph/0606049*, 2006.
- [39] A. Acín, N. Gisin, and L. Masanes, “From bell’s theorem to secure quantum key distribution,” *Phys. Rev. Lett.*, vol. 97, p. 120405, 2006.
- [40] W. Maurer and C. Silberhorn, “Passive decoy state quantum key distribution: Closing the gap to perfect sources,” *arXiv:quant-ph/0609195*, 2006.
- [41] Y. Adachi, T. Yamamoto, M. Koashi, and N. Imoto, “Simple and efficient quantum key distribution with parametric down-conversion,” *arXiv:quant-ph/0610118*, 2006.
- [42] Q. Wang, X.-B. Wang, and G.-C. Guo, “Practical decoy-state method in quantum key distribution with a heralded single-photon source,” *Physical Review A*, vol. 75, p. 012312, 2007.
- [43] R. Ursin, F. Tiefenbacher, T. Schmitt-Manderbach, H. Weier, T. Scheidl, M. Lindenthal, B. Blauensteiner, T. Jennewein, J. Perdigues, P. Trojek, B. Oemer, M. Fuerst, M. Meyenburg, J. Rarity, Z. Sodnik, C. Barbieri, H. Weinfurter, and A. Zeilinger, “Free-space distribution of entanglement and single photons over 144 km,” *arXiv:quant-ph/0607182*, 2006.
- [44] D. Gottesman and H.-K. Lo, “Proof of security of quantum key distribution with two-way classical communications,” *IEEE Transactions on Information Theory*, vol. 49, 2003.
- [45] K. Gerd, H. Vollbrecht, and F. Verstraete, “Interpolation of recurrence and hashing entanglement distillation protocols,” *Phys. Rev. A*, vol. 71, p. 062325, 2005.

- [46] X. Ma, C.-H. F. Fung, F. Dupuis, K. Chen, K. Tamaki, and H.-K. Lo, “Decoy state quantum key distribution with two-way classical post-processing,” *Phys. Rev. A*, vol. 74, p. 032330, 2006.
- [47] M. Aspelmeyer, T. Jennewein, M. Pfennigbauer, W. R. Leeb, and A. Zeilinger, “Long-distance quantum communication with entangled photons using satellites,” *IEEE Journal of Selected Topics in Quantum Electronics, special issue on Quantum Internet Technologies*, vol. 9, pp. 1541–1551, 2003. [arxiv.org/quant-ph/0305105](https://arxiv.org/abs/quant-ph/0305105).
- [48] P. Villoresi, F. Tamburini, M. Aspelmeyer, T. Jennewein, R. Ursin, C. Pernechele, G. Bianco, A. Zeilinger, and C. Barbieri, “Space-to-ground quantum-communication using an optical ground station: a feasibility study,” *SPIE proceedings Quantum Communications and Quantum Imaging II conference in Denver*, 2004.
- [49] P. Kok and S. L. Braunstein, “Postselected versus nonpostselected quantum teleportation using parametric down-conversion,” *Phys. Rev. A*, vol. 61, p. 042304, 2000.
- [50] H.-K. Lo, H.-F. Chau, and M. Ardehali, “Efficient quantum key distribution scheme and a proof of its unconditional security,” *Journal of Cryptology*, vol. 18, no. 2, pp. 133–165, 2005.
- [51] G. Brassard and L. Salvail, “Secret-key reconciliation by public discussion,” in *Advances in Cryptology EUROCRYPT ’93*, Springer-Verlag, Berlin, 1993.
- [52] M. Koashi, “Efficient quantum key distribution with practical sources and detectors,” *arXiv:quant-ph/0609180*, 2006.
- [53] H.-K. Lo and J. Preskill, “Security of quantum key distribution using weak coherent states with nonrandom phases,” *arXiv:quant-ph/0610203*, 2006.
- [54] M. Koashi, “Unconditional security proof of quantum key distribution and the uncertainty principle,” *J. Phys. Conf. Ser.*, vol. 36, p. 98, 2006.
- [55] B. Kraus, N. Gisin, and R. Renner, “Lower and upper bounds on the secret-key rate for quantum key distribution protocols using one-way classical communication,” *Phys. Rev. Lett.*, vol. 95, p. 080501, 2005.
- [56] N. Lütkenhaus, “Quantum key distribution: theory for application,” *Appl. Phys. B*, vol. 69, pp. 395–400, December 1999.
- [57] Then the final key length is 15 bits. One should also consider the cost in the authentication procedure. Thus this is a reasonable cut off point.